JOURNAL OF MATERIALS SCIENCE **40** (2005) 3651 – 3657

The shock properties of a La_2O_3 filled silicate glass

J. C. F. MILLETT*
Royal Military College of Science, Cranfield University, Shrivenham, Swindon, SN6 8LA. UK
E-mail: j.c.f.millett@cranfield.ac.uk

N. K. BOURNE
School of Mechanical, Aerospace and Civil Engineering, The University of Manchester, North Campus, Sackville Street, Manchester, M60 1QD, UK

A survey of the shock properties of the silicate glass, LACA has been carried out using manganin stress gauges. The principal Hugoniot has been measured and found to have significantly higher values than for other common silicate glasses. Gauges mounted on the rear of the target (supported with a block of polymethylmethacrylate) show reloading signals superimposed on the main compressive shock pulse. This has been interpreted as evidence of dynamic compressive failure (the failure wave or front). Manganin gauges mounted so as to be sensitive to the lateral component of stress support this hypothesis. Finally, failure front velocities , measured using known lateral gauge separations increase with increasing shock stress, tending towards the shear wave speed.

1. Introduction

The properties of materials under high-loading rate conditions have been of interest for a number of years. Traditionally, this has been driven by the military by their need to gain an understanding of materials for armour and armour defeat applications. However, more recently, interest has come from other areas such as the automotive industry (crashworthiness testing) aerospace (foreign object damage in jet turbine engines and structural members) and satellite protection. Unfortunately, the impact of a real object (such as a bird) onto a real target (an aerofoil) yields a complex stress state where all conditions of strain may apply under the impact site. This makes a rigourous analysis of that impact near impossible, and hence material response under impact conditions is generally performed using a simpler loading geometry, such that materials properties may be extracted and used in constitutive models to predict an actual event. One such technique is that of plate impact. In this situation, a flat and parallel flyer plate of a known material is impacted at high velocity (>100 m s^{-1}) onto an equally flat and parallel plate of the material of interest. This generates a planar shock front, behind which conditions of one-dimensional strain prevail. Under these circumstances, the strain (ε) is accommodated down the impact axis (denoted as x), whilst the strains perpendicular to it (y and z) are zero due to inertial confinement. As a consequence, a three dimensional state of stress (σ) exists, thus,

$$\varepsilon_x \neq \varepsilon_y = \varepsilon_z = 0 \quad \text{and} \quad \sigma_x \neq \sigma_y = \sigma_z \neq 0. \quad (1)$$

For a more complete description of shock loading, the reader is directed to the review article of Davison and Graham [1].

The shock properties of silicate glasses, measured in one-dimensional plate impact have been a source of interest for some time. These have included open-structured materials such as fused silica [2, 3] and borosilicate [4], partially filled glasses such as soda-lime [5, 6], and high-density filled glasses such as DEDF (type D, Extra Dense Flint) [7, 8]. Previous work [9] has shown that this variation in structure has a profound effect upon the shock properties of these materials. In borosilicate, the shock is highly ramped, due to the collapse of the open structure to a denser state, whilst in contrast, DEDF displays a sharp jump to its Hugoniot Elastic Limit (HEL—the one-dimensional yield stress), in a manner similar to polycrystalline ceramics [10]. The mechanical shock behaviour of the partially filled soda-lime is intermediate between borosilicate and DEDF.

In the past decade, one of the more interesting features to emerge is that of the failure wave. This was first observed by Razorenov *et al*. [11] who detected small reload signals superimposed upon rear-surface velocity traces taken from K19 glass (similar to soda-lime). This they interpreted as a reflection of the release from the rear of the target interacting with a slower moving front behind the main shock. As that reflection was compressive in nature, they deduced that the material behind that front must have a lower shock impedance than ahead of it. They thus suggested that the material behind that

* Author to whom all correspondence should be addressed.

front may have fractured, and called it the failure wave. Some years earlier, Nikolaevskii [12] had proposed just such a mechanism. Brar *et al.* [6, 13] provided further confirmation of the failure wave, showing that the spall strength (dynamic tensile strength) reduced from a finite value ahead of the failure wave to zero behind it. They also demonstrated that the lateral component of stress (σ_y) increased markedly behind the failure wave. This was explained in terms of the shear strength (τ) reducing behind the failure wave, since,

$$2\tau = \sigma_x - \sigma_y, \tag{2}$$

where σ_x is the longitudinal stress. Finally, Bourne *et al.* [14] were able to visualise failure waves in soda-lime glass using high-speed-photography. Here it was observed that the failure wave existed as a front behind which the material became completely opaque.

The origins of failure waves have been investigated by a number of workers. Kanel and his colleagues [15, 16] have suggested that failure is initiated at the impact surface due to the presence of flaws providing a source of localised tension. Rasier *et al.* [17] made an attempt to confirm this by performing spallation experiments on glass samples with differing degrees of impact surface finish. Their results indicated that no difference in failure wave propagation occurred, leading them to suggest that failure waves were a bulk rather than a surface phenomenon. In contrast, Bourne *et al.* [18, 19] shock loaded glass target assemblies with internal interfaces finished to varying levels of grinding and polishing. Failure was observed to be re-initiated at that interface, occurring more quickly with increasing levels of damage. Various attempts have also been made to model failure waves. Clifton [20] did so as a propagating phase boundary with some degree of success, although he admitted his model was far from complete. Feng [21] suggested that the failure wave consist of a moving front of damage due to the simultaneous formation of microfissuring, shear dilatency and void collapse. This was used to generate a model that was used in comparison with the experimental results of Kanel *et al.* [15] and Bourne and Rosenberg [22] with a reasonable degree of success. He also pointed out that in using this method, the failure wave could not be considered as a mechanical wave in a similar way to a shock front. As such, the term "failure front" will be applied from this point on to this feature.

Lateral stress measurements have been made for borosilicate, soda-lime and filled lead glasses [23], where we have shown that the shear strengths of all three materials lie on the same unfailed and failed curves, when plotted against longitudinal stress. These results suggest that the silica network, common to all, controls the strength during shock loading. It is possible that this will apply to other silicate glasses as well. Therefore the work discussed in this paper describes the results from plate impact experiments on a fourth silicate glass, LACA.

2. Experimental

Plate impact experiments were performed using a 5 m long, 50 mm bore single stage gas gun. Manganin stress gauges (MicroMeasurements type LM-SS-125CH-048) were placed in longitudinal orientation either between 10 mm tiles to measure the internal stress (the embedded configuration), or supported on the back of the tile with a 12 mm block of polymethylmethacrylate (PMMA) in the back-surface configuration. The shock impedances of PMMA, the epoxy gauge backing and the epoxy adhesive are nearly identical, and thus the rise-time of the gauge in this configuration will be much faster than when it is embedded between plates of the target material. In this situation, the signal has to ring-up in the epoxy layer between them. Thus in the back-surface configuration, details in the rise of the stress pulse may be observed that could be missed with an embedded gauge. Voltage—time data from the gauges was converted to stress—time, according to the calibration of Rosenberg *et al.* [24].

Lateral stresses were also measured, using a different manganin stress gauge (MicroMeasurements type J2M-SS-580SF-025). In this series of experiments, 19 mm thick tiles of LACA were sectioned in half, and the gauges introduced at known distances from the impact face (3 and 7 mm) to an accuracy of ca. 0.2%. As these gauges were used to measure the failure front velocity, greater accuracy was needed. However, as the initial part of the shock pulse would travel at the longitudinal elastic wave speed (measured acoustically) which is known, the temporal spacing of the gauges could be measured from the gauge traces, and thus the physical spacing of the gauges determined, which are then used in the failure front velocities. The targets were reassembled using a slow setting epoxy resin, and held in a special jig for a minimum of 12 h. Impact faces were lapped prior to testing. Lateral stresses from the gauges were determined using the analysis of Rosenberg and Partom [25], with a modification that did not require prior knowledge of the impact conditions [26]. Specimen configurations and gauge placements are presented in Fig. 1.

For specimens in the embedded configuration, 3 mm copper flyer plates were impacted onto 10 mm targets at velocities of 257, 441, 672 and 848 m s^{-1}. In the back-surface configuration, 6 mm copper flyer plates were fired at a velocity of ca. 652 m s^{-1} at specimen thicknesses of 5, 8 and 12 mm. For experiments measuring the lateral stresses, 10 mm copper flyer plates were impacted at velocities of 356, 629 and 789 m s^{-1}. Impact velocities were measured by the shorting of sequentially mounted pairs of pins to an accuracy of $\pm 0.5\%$. Acoustic properties were measured using 5 MHz quartz transducers, in both longitudinal and shear orientation, using a Panametrics 5052PR pulse receiver.

3. Materials data

The composition of LACA and other silicate glasses are shown in Table I. The elastic properties of LACA are presented in Table II. As a comparison, the properties of borosilicate, soda-lime and DEDF are also included.

4. Results and Discussion.

Stress histories from the embedded gauges are presented below in Fig. 2.

TABLE I Composition of silicate glasses (weight percent)

	LACA	Soda-Lime	Borosilicate	DEDF
SiO_2	18.42	72.6	80.6	27.3
Al_2O_3		1.0	2.2	
Na_2O		13.0	4.2	
K_2O		0.6		1.5
PbO				71.0
La_2O_3	33.28			
MgO		3.94	0.05	
CaO	19.84	8.4	0.1	
BaO	1.01			
Fe_2O_3		0.11	0.05	
As_2O_3				0.1
B_2O_3	25.34		12.6	
ZrO_2	2.01			

TABLE II Acoustic properties of silicate glasses

Material	c_L (mm μs^{-1})	c_s (mm μs^{-1})	ρ_0 (g cm^{-3})	ν
LACA	6.26 ± 0.01	3.42 ± 0.01	3.52 ± 0.05	0.29
Soda-lime	5.84 ± 0.01	3.46 ± 0.01	2.49 ± 0.05	0.23
Borosilicate	6.05 ± 0.01	3.69 ± 0.01	2.23 ± 0.05	0.20
DEDF	3.49 ± 0.01	2.02 ± 0.01	5.18 ± 0.05	0.25

c_L – Longitudinal sound speed.
c_S – Shear sound speed.
ρ_0 – Ambient density.
ν-Poisson's ratio.

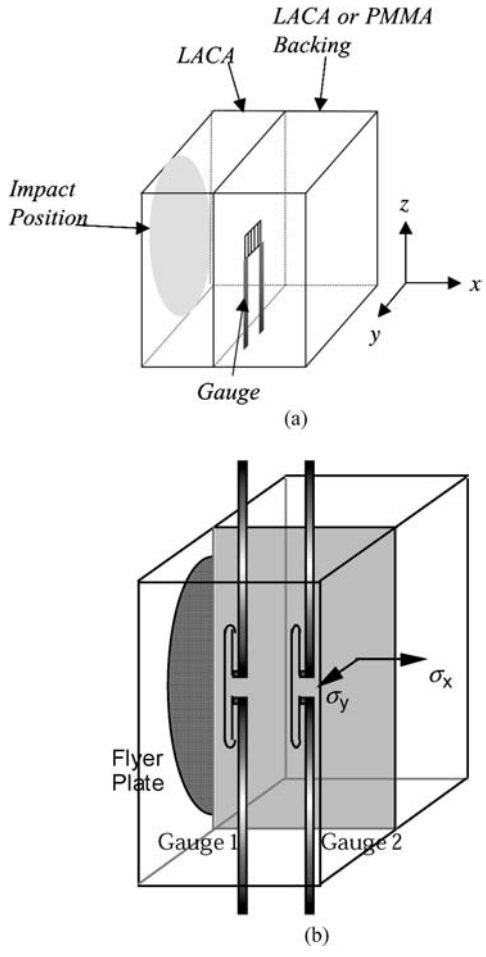

Figure 1 Specimen configurations and gauge placements. (a) Longitudinal gauges (b) Lateral gauges.

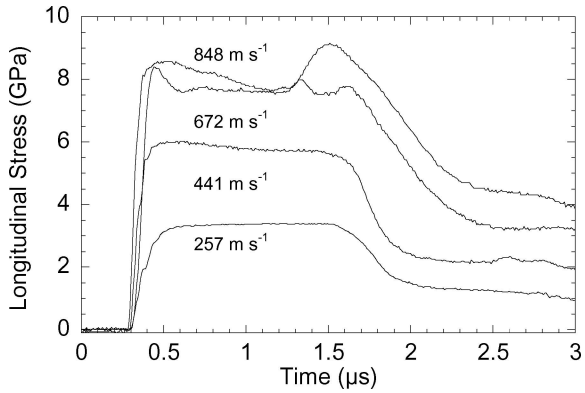

Figure 2 Embedded longitudinal gauge traces for LACA. Flyer plates are 3 mm copper.

It can be seen that all stress pulses are ca. 1.25 μs in duration, corresponding to a double transit time across a 3 mm copper flyer plate. However, it can be seen that as impact velocity increases, the response of LACA becomes increasingly complex. At 257 m s^{-1}, the shock pulse consists of a simple step, with a maximum amplitude of 3.4 GPa. At 441 m s^{-1}, a slight relaxation behind the shock front, from 6 to 5.5 GPa is observed. As the impact velocity increases still further, to 672 m s^{-1}, a distinct overshoot is observed before the stress settles to a near constant level of 7.6 GPa. Finally, at the highest impact velocity of 848 m s^{-1}, an initial stress of 8.5 GPa is reached, before a slow relaxation to ca. 7.5 GPa. However, stress then rises approximately 0.5 μs after to reach ca. 9 GPa before releases enter the gauge location. Normally, one would expect a simple plateau behind the shock front but the relaxations observed in the embedded gauge traces may be an indication of stress relief due to failure (i.e. the failure front) reducing the longitudinal stress. Relaxations in longitudinal stress behind the shock front measured by embedded gauges have been observed on other silicate glasses, notably DEDF [7] where it was suggested that this be due to the influence of the failure wave. However, such a hypothesis does not explain all features observed in the longitudinal stress traces such as the reload observed at an impact velocity of 848 m s^{-1}.

Three shots were carried out in the back-surface configuration, using 6 mm copper flyer plates at a velocity of 652 m s^{-1}, impacted on to targets 5, 8 and 12 mm thick, The resultant traces are shown below in Fig. 3. All three traces share common features, these being an initial rapid rise in stress to ca. 3 GPa, before dropping to ca. 2.4 GPa. In all three traces, this initial peak is identical. This would suggest that this feature may be a gauge artefact; if it were stress related, it might be expected that its duration would depend upon the thickness of the sample. In contrast, once the measured stress has dropped to 2.4 GPa, the duration is dependent on thickness, before rising to 3.2 GPa. In the traces labelled 5 and 12, it does so as a step, whilst for the trace labelled 8, the rise is of a lesser gradient. Stresses measured in PMMA may be converted to in-material stresses through knowledge of the shock impedances

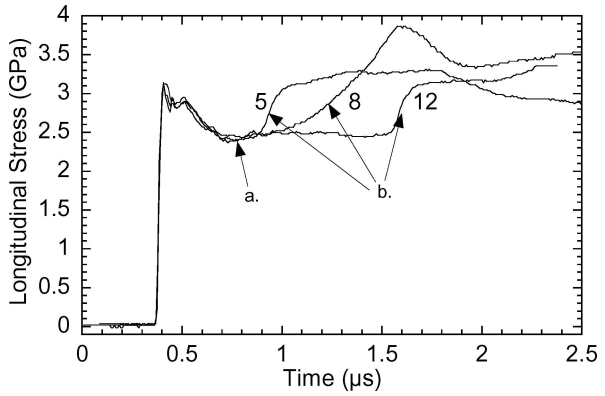

Figure 3 Back surface gauge traces for 5, 8 and 12 mm LACA. 6 mm copper flyer plates at ca. 652 m s^{-1}.

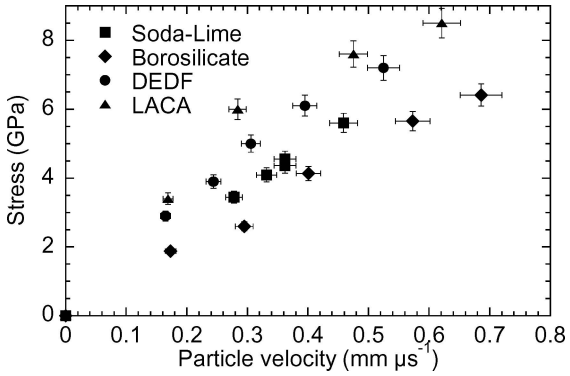

Figure 5 Hugoniots of four silicate glasses.

(Z) of LACA and PMMA,

$$\sigma_L = \frac{Z_L + Z_P}{2Z_P}\sigma_P, \tag{3}$$

where,

$$Z = \rho_0 U_s, \tag{4}$$

ρ_0 and U_s are the ambient density and shock velocities at the measured stress and the subscripts L and P refer to LACA and PMMA respectively. In the case of LACA, we have used the elastic impedance since these parameters are unknown, substituting the longitudinal sound speed instead. This will result in a small error of approximately 5% in the final calculated stress. From Equation 3, in-material stresses of 7.4 GPa after the first peak (marked a.) and 8.9 GPa (marked b.) after the arrival of the second rise in stress are observed. Only the lower value agrees with the measured Hugoniot shown in Fig. 4, and thus it would seem unlikely that the second rise in stress is due to the inelastic part of the stress pulse. A second and more likely possibility is that this is the result of a reload signal. In this scenario, the shock is reflected from the LACA/PMMA interface as a partial release. It travels back into the target, where it interacts with a slower moving front from which it is partially reflected back to the gauge location as a recompression. As it is recorded at the gauge location as a reload signal, the material behind the front must have a reduced shock impedance. Such behaviour has been observed in other glasses [11], and interpreted as the material behind that front fracturing. However, the magnitude of that reload is usually much smaller than is observed in LACA. However, very recently, we have noted similar behaviour in the back surface response of a glass-ceramic [27]. It was suggested in that work that an impedance drop across the failure front of ca. 60% was necessary to cause such a large reload signal in the back surface gauge traces. The differences in the nature of the reload signal between the traces labelled 5 and 12, and the trace labelled 8 may have been due to an unknown flaw in that particular sample initiating failure in a different manner to the other two samples. However, despite this, the basic response is still largely the same.

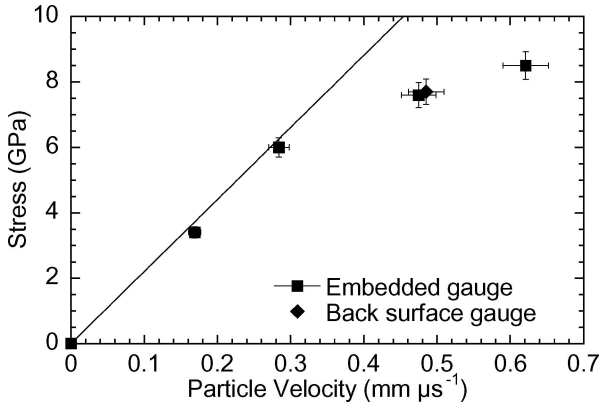

Figure 4 Hugoniot of LACA in stress—particle velocity space. The straight line is the elastic response according to Equation 4.

In Fig. 4, we present the Hugoniot of LACA in stress-particle velocity (u_p – the velocity of material flow behind the shock front) space. This was determined from the maximum stresses measured in Fig. 2, with particle velocities deduced from impedance matching techniques. Also included is the steady stress value from Fig. 3, converted from a value measured in PMMA to an internal stress using Equation 2.

The straight line fit is according to the elastic impedance, thus,

$$\sigma_x = \rho_0 c_L u_p. \tag{5}$$

As can be seen, the measured Hugoniot data agree with the calculated elastic response up to ca. 6 GPa, before deviating to a lower gradient, thus implying that the HEL of this glass occurs at this point. Also observe that the stress point calculated from the back surface technique (Fig. 4) is in close agreement with those points measured with gauges mounted internally.

As a comparison, we show the Hugoniot of LACA in combination with those of the three other common silicate glasses, soda-lime, borosilicate and DEDF [28]. It is clear that the steepness of the Hugoniots rank from borosilicate with the shallowest, through soda-lime, DEDF and finally LACA. This is the response that would be expected from inspection of the elastic impedances shown in Table II.

In Fig. 6, representative gauge traces measuring the lateral stress response (ca. 8.2 GPa) are presented, with

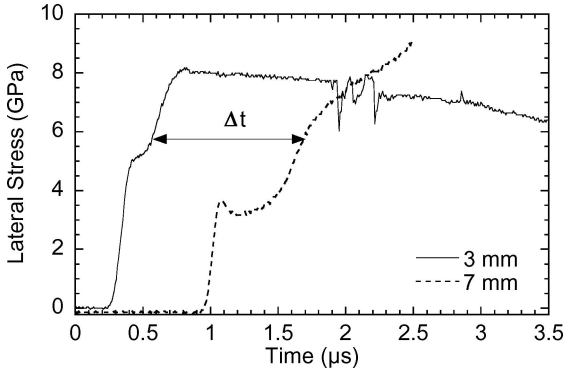

Figure 6 Lateral gauge traces at positions 3 and 7 mm from the impact face. The impact conditions are 10 mm copper flyer at 789 m s^{-1}, σ_x = 8.2 GPa.

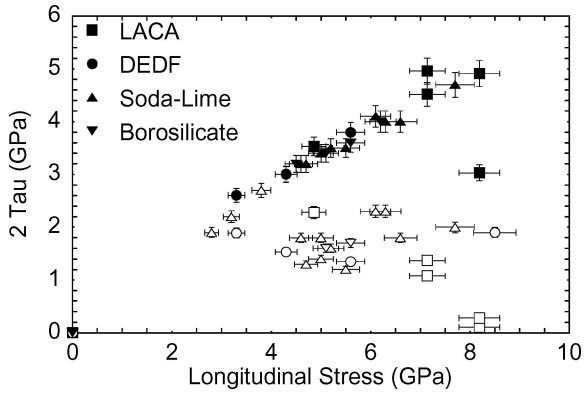

Figure 8 Shear strengths of four silicate glasses. Closed symbols denote strength ahead of the failure wave; open symbols denote strength behind the failure front.

the gauges mounted 3 and 7 mm from the impact face. Observe that both traces show the two-step nature that is indicative of the failure front process. The duration of the stress at the first step is greater at 7 mm than at 3 mm, thus showing that the second part of the lateral stress signal (i.e. the failure wave) travels slower than the initial part. Also observe that the height of the first step at 3 mm is higher than the corresponding stress level at 7 mm. From Equation 2, this indicates that the shear strength close to the impact face is lower than in the body of the specimen. A similar response has been seen in soda-lime glass [29], where it was suggested that the lapping process necessary after assembly of the target may introduce flaws at the impact surface which could initiate failure that in turn would result in a small reduction in shear strength. The lateral stresses ahead of and behind the failure wave, in combination with the Hugoniot stresses from known impact conditions, were used to generate the variation of shear strength with impact stress from Equation 2. The results are presented in Fig. 7.

Ahead of the failure front, measured shear stresses are in agreement with the calculated response, according to,

$$2\tau = \frac{1-2\nu}{1-\nu}\sigma_x, \tag{6}$$

even above the proposed HEL of ca. 6 GPa, determined from Fig. 4. This response has been observed in other

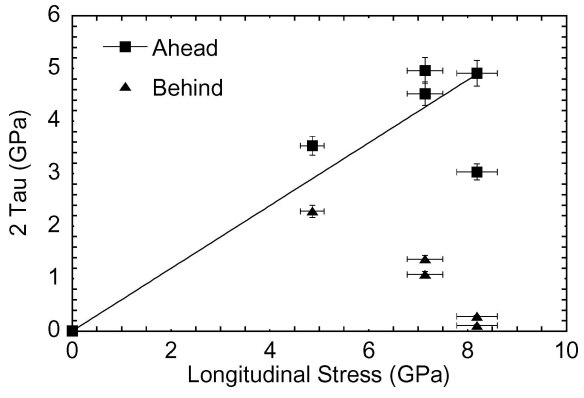

Figure 7 Shear strengths ahead and behind the failure front in LACA. The straight line is a fit according to Equation 5.

silicate glasses [23, 28], and is an indication that the response of these materials does not conform to the elastic—inelastic yield response seen in metallic systems. Behind the failure front, shear strength decreases with increasing impact stress until at ca. 8 GPa, it is effectively zero. This is in contrast to other silicate glasses such as soda-lime, borosilicate and DEDF, where not only shear strength behind the failure front maintained a constant value, but was near identical in all three materials [23]. This is shown in Fig. 8, in comparison with the results of LACA.

It can be seen that the unfailed strength of LACA agrees with the unfailed strength of the other three glasses [23], despite the fact that they have very different structures (open silicate network for borosilicate to filled with 70% lead oxide by weight in DEDF), acoustic properties (Table II) and Hugoniots (Fig. 4). It was suggested that this be due to the common silicate network in all three materials being the controlling factor of the strength during shock loading. Given that LACA agrees with this pattern is further evidence that this hypothesis is correct. The situation with the failed strengths is more interesting. From Fig. 8 and previous work [23, 28] the failed strengths of borosilicate, soda-lime and DEDF are all similar, whilst that of LACA, whilst initially similar to the previous materials at lower stresses, drops to near zero at a higher impact stress of ca. 8 GPa. In the three former materials, that a residual shear strength is maintained, even after fracture could be explained due to the resistance of an inertially confined powder to flow. The precise nature of this resistance will be dependent upon a number of factors, included size of fractured particles, degree of inertial confinement, and the degree of connectivity between cracks. It is thus possible to forsee a situation where, as impact stress increases, the cracking becomes more intense, and thus the resultant particles reduce in size, thus making overall resistance to flow, and hence the resultant shear strength less. However, work by Radford *et al.* [30] in high density glasses indicates that the failed shear strengths increase above an impact stress of ca. 8 GPa, citing fragment interlocking. As our own measurements were only performed to a maximum impact stress of 8 GPa, we cannot comment on whether LACA would show a similar response.

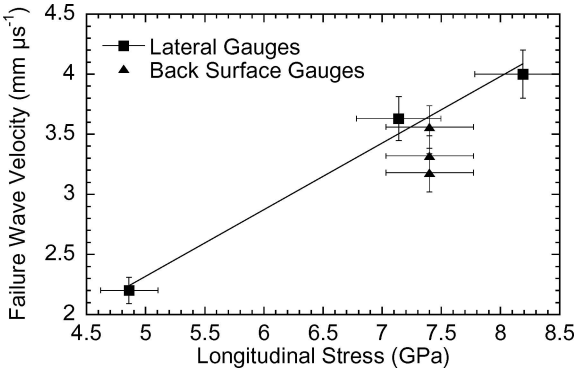

Figure 9 Failure front velocities in LACA as a function of imposed shock stress.

From Fig. 6, it can be seen that gauges were placed at two different distances from the impact face, these being 3 and 7 mm. By doing so, this allowed us to determine the failure front velocity (c_{fail}) from known temporal separations of the relevant parts of the signals (denoted Δt) and the spacing of the gauges (d). These were calculated according to,

$$c_{\text{fail}} = \frac{d}{t}\left(1 - \frac{u_p}{U_s}\right), \tag{7}$$

where U_s (the shock velocity) has been substituted for c_L (the elastic wave speed). The derivation of Equation 6 can be found in a previous paper [29]. The results are presented in Fig. 9.

We have also included failure front velocities determined from the back-surface traces shown in Fig. 3. It can be seen that, given the assigned errors, the degree of agreement between the two methods is reasonable, and thus gives us confidence that the observed reload signals seen in Fig. 3 and the two step nature of the lateral stress traces in Fig. 6 are due to the failure wave process. One final feature worthy of note concerns the failure wave velocity at the highest impact stress (4.0 mm μs^{-1}). Obviously the failure front, as it is slower than the main shock will be moving into material that is already compressed, and moving at the particle velocity. From the impact conditions of this shot, the particle velocity for this particular shot was 0.584 mm μs^{-1}. Subtracting this from the measured failure front velocity gives a value of 3.42 mm μs^{-1}. This is identical to the measured shear wave velocity (Table II). The longitudinal stress is expressed in terms of the hydrostatic pressure (P) and shear strength (τ) through the relation,

$$\sigma_x = P + \frac{4}{3}\tau. \tag{8}$$

Thus it can be seen that whilst the overall loading is compressive, there is a significant shear component that contributes to the failure. Under these conditions, the failure will occur via shear cracking (mode II). It is generally accepted that such cracks cannot travel faster than the shear wave speed; the fact that the maximum failure wave speed measured in this study, taking the imposed particle velocity into account would seem to confirm this.

5. Conclusions

Plate impact experiments have been carried out on the La_2O_3 filled silicate glass, LACA. The Hugoniot has been measured and compared to other silicate glasses, and been shown to have higher values than borosilicate, soda-lime and DEDF, in accordance with the measured values of elastic impedance. Reload signals in the back-surface traces have been interpreted as reflections of the release from failure front fronts. Lateral stress gauge measurements have confirmed this hypothesis. Results show that the unfailed shear strengths of LACA are the same as the other glasses. We believe this to be due to the common silica network found in all four materials. In contrast, the failed strengths decrease as impact stress increases. Finally, failure front velocities have been shown to increase with impact stress, tending towards the shear wave speed.

References

1. L. DAVISON and R. A. GRAHAM, *Phys. Reports* **55** (1979) 255.
2. J. WACKERLE, *J. Appl. Phys.* **33** (1962) 922.
3. H. SUGIURA, K. KONDO and A. SAWAOKA, *ibid.* **52** (1981) 3375.
4. J. CAGNOUX, in "Shock Waves in Condensed Matter—1981," edited by W. J. Nellis, L. Seaman and R. A. Graham (AIP Press, Menlo Park, Ca, 1982) p. 392.
5. S. J. BLESS, N. S. BRAR, G. KANEL and Z. ROSENBERG, *J. Am. Ceram. Soc.* **75** (1992) 1002.
6. N. S. BRAR, Z. ROSENBERG and S. J. BLESS, *J. Physique IV* **Colloque C3** (1991) 639.
7. N. K. BOURNE, J. C. F. MILLETT and Z. ROSENBERG, *Proc. R. Soc. Lond. A* **452** (1996) 1945.
8. *Idem.*, *J. Appl. Phys.* **80** (1996) 4328.
9. N. K. BOURNE, Z. ROSENBERG and A. GINSBERG, *Proc. R. Soc. Lond. A* **452** (1996) 1491.
10. N. H. MURRAY, N. K. BOURNE and Z. ROSENBERG, *J. Appl. Phys.* **84** (1998) 4866.
11. S. V. RAZORENOV, G. I. KANEL, V. E. FORTOV and M. M. ABASEMOV, *High Press. Res.* **6** (1991) 225.
12. V. N. NIKOLAEVSKII, *Int. J. Engng. Sci.* **19** (1981) 41.
13. N. S. BRAR, S. J. BLESS and Z. ROSENBERG, *Appl. Phys. Letts.* **59** (1991) 3396.
14. N. K. BOURNE, Z. ROSENBERG and J. E. FIELD, *J. Appl. Phys.* **78** (1995) 3736.
15. G. I. KANEL, S. V. RASORENOV and V. E. FORTOV, in "Shock Compression of Condensed Matter," edited by S. C. Schmidt, R. D. Dick, J. W. Forbes and D. G. Tasker (Eleseiver Science Publishers BV, 1991) p. 451.
16. G. I. KANEL, A. A. BOGATCH, S. V. RAZORENOV and Z. CHEN, *J. Appl. Phys.* **92** (2002) 5045.
17. G. F. RAISER, J. L. WISE, R. J. CLIFTON, D. E. GRADY and D. E. COX, *ibid.* **75** (1994) 3862.
18. N. K. BOURNE, J. C. F. MILLETT and Z. ROSENBERG, *ibid.* **81** (1997) 6670.
19. N. BOURNE and J. MILLETT, *Proc. R. Soc. Lond. A* **459** (2000) 2673.
20. R. J. CLIFTON, *Appl. Mech. Rev.* **46** (1993) 540.
21. R. FENG, *J. Appl. Phys.* **87** (2000) 1693.
22. N. K. BOURNE and Z. ROSENBERG, in "Shock Compression of Condensed Matter-1995," edited by S. C. Schmidt and W. C. Tao (American Institute of Physics, Melville, NY, 1996) p. 567.
23. N. K. BOURNE, J. C. F. MILLETT and J. E. FIELD, *Proc. R. Soc. Lond. A* **455** (1999) 1275.
24. Z. ROSENBERG, D. YAZIV and Y. PARTOM, *J. Appl. Phys.* **51** (1980) 3702.
25. Z. ROSENBERG and Y. PARTOM, *ibid.* **58** (1985) 3072.
26. J. C. F. MILLETT, N. K. BOURNE and Z. ROSENBERG, *J. Phys. D. Appl. Phys.* **29** (1996) 2466.

27. I. M. PICKUP, J. C. F. MILLETT and N. K. BOURNE, in "Shock Compression of Condensed Matter—2003," edited by M. D. Furnish, Y. M. Gupta and J. W. Forbes (AIP Press, Melville, NY, 2004) p. 751.
28. N. BOURNE, J. MILLETT, N. MURRAY and Z. ROSENBERG, *J. Mech. Phys. Solids* **46** (1998) 1887.
29. J. C. F. MILLETT and N. K. BOURNE, *J. Appl. Phys.* **95** (2004) 4681.
30. D. D. RADFORD, W. G. PROUD and J. E. FIELD, in "Shock Compression of Condensed Matter—2001," edited by M. D. Furnish, N. N. Thadhani and Y. Horie (AIP Press, Melville, NY, 2002) p. 807.

Received 22 October 2004
and accepted 28 February 2005